JOURNAL OF AIRCRAFT
Vol. 33, No. 4, July–August 1996

Experimental Study of Vortex Flow Control on Double-Delta Wings Using Fillets

Sheshagiri K. Hebbar,* Max F. Platzer,† and Abdullah M. Alkhozam‡
U.S. Naval Postgraduate School, Monterey, California 93943

An experimental investigation of vortex flow control through small geometry modifications (fillets) at the strake/wing junction of a cropped, double-delta wing model with sharp leading edges was conducted in a water tunnel at a model Reynolds number of 1.875×10^4. The fillets increased the wing area of the baseline model by 1%. The main focus of this study was to evaluate the effects of fillets on vortex core trajectories, interactions, and breakdown (bursting) on the leeward surface at high angles of attack (AOAs), using the dye-injection technique. Comparison of test results for different fillet shapes indicates delay in both vortex interaction and breakdown at high AOAs, particularly for the diamond-fillet shape. The vortex trajectory data for the diamond-fillet shape clearly imply lift augmentation, thus supporting the concept of flow control using fillets. The vortex breakdown data indicate lift augmentation for both the static and dynamic cases.

Nomenclature

C = wing centerline chord
$d\alpha/dt$ = pitch rate, rad/s
k = reduced pitch rate of the wing, $(d\alpha/dt)C/2U_\infty$
Re = freestream Reynolds number, $\rho_\infty U_\infty C/\mu_\infty$
U_∞ = freestream velocity
X_b = streamwise strake–vortex burst location
X, Y, Z = wing fixed, rectangular coordinates of any point on vortex core trajectory, with X measured streamwise along the wing centerline from the apex, Y measured spanwise outboard from the centerline, and Z measured perpendicular to and away from the wing upper surface
α = angle of attack, deg
μ_∞ = dynamic viscosity of water
ρ_∞ = density of water

Introduction

THE design of future combat aircraft will have to incorporate features providing enhanced fighter maneuverability. High angle-of-attack (AOA) flight is limited by the vortex breakdown phenomenon and by the onset of vortex asymmetry. As a result, large undesired forces and moments can occur that may lead to departure from controlled flight, and therefore attention has to be paid to high-rate pitch-up problems, lateral and directional instability problems, and roll and yaw control problems. The forebody of the fuselage, the strakes, and canards have a strong influence on vortex developments and on lateral and directional stability.

A good understanding of the basic phenomenon of vortex-dominated flows, the ability to predict such flows, and control them through vortex manipulation are therefore crucial to enhance aircraft maneuverability. In the 1960s, SAAB of Sweden used canards to delay the separation on the upper surface of the main wing of the Viggen Fighter.[1] In the 1970s, the use of leading-edge extensions (LEXs) or strakes was developed and successfully applied to F-16 and F/A-18 aircraft. Lamar[2] suggested that a significant rolling moment could be obtained for control purposes by reducing the vortex lift on one side of a wing and maintaining the vortex lift on the other side. In fact, as early as the 1950s, the use of asymmetric-edge shape effects was suggested to achieve roll control of low-aspect ratio wings at high AOAs (Ref. 3). Since the vortical flow dominates the lift at high AOAs, there has been a resurgence of research effort to control flow through vortex manipulation. The use of dynamic lift and dynamic flow control by vortex manipulation has now been recognized as an attractive possibility to enhance modern aircraft maneuverability. This control concept relies on modifying the vortex at its point of origin near the shedding point (such as at the junction of the strake and wing of a double-delta wing).

Both pneumatic and mechanical devices are being investigated as candidates for vortex manipulation. Detailed reviews of vortex flow control through geometry modification appear in Refs. 1, 4, and 5. A brief review of vortex control concepts is given in Ref. 6. The recent numerical study by Kern[6] on vortex flow control through small geometry modifications (fillets) at the strake/wing junction of a double-delta wing suggested that the use of fillets could enhance the lift by 13.6% at low AOA and 17.9% at high AOA with a slight improvement in lift-to-drag ratio. It even suggested that the fillets may be good candidates for roll control devices. Note that the fillets are envisioned as being deployable on demand at the junction of the strake and the wing during air combat maneuvers or carrier landing approach. A symmetric deployment of the fillets would result in enhanced lift and longitudinal control, whereas an asymmetric deployment would provide lateral–directional control. Thus, pending further studies and experimental verification, the concept of flow control by small deployable fillets at the junction of a double-delta wing appears promising during nonmaneuver (static pitch) conditions.

A double-delta wing is a strake/wing configuration that has geometric characteristics similar to those of a delta wing except for a discontinuity or kink in its leading edge. The flow over a double-delta wing is similar to that over a delta wing, but is more complex because of the additional phenomenon of vortex interaction between the strake vortex and the wing vortex. Wind-tunnel investigations of double-delta wings

Presented as Paper 95-0649 at the AIAA 33rd Aerospace Sciences Meeting and Exhibit, Reno, NV, Jan. 9–12, 1995; received May 21, 1995; revision received Feb. 28, 1996; accepted for publication March 1, 1996.

*Adjunct Professor, Department of Aeronautics and Astronautics. Associate Fellow AIAA.

†Professor, Department of Aeronautics and Astronautics. Associate Fellow AIAA.

‡Graduate Student, Department of Aeronautics and Astronautics; currently, Lieutenant, Kuwait Air Force. Member AIAA.

have been reported in Refs. 7–9, and water-tunnel investigations in Refs. 10 and 11. Computed solutions[6,12,13] of the Navier–Stokes equations for the flow about a 76-/40-deg double-delta wing seem to predict the interaction and breakdown of the strake and wing vortices and surface pressure levels reasonably well at low AOAs. There are some disagreements in the interaction and bursting data between the water-tunnel tests, wind-tunnel tests, and the numerical predictions. The water-tunnel data of Hebbar et al.[11] indicate that, with increasing AOA, the strake/wing interaction moves upstream until the AOA is large enough to cause bursting of the strake vortex even before the interaction with the wing vortex. These observations are in general agreement with those reported in water-tunnel/wind-tunnel studies.[8–10] The AOA range for coiling-up of the vortices is narrow (10–25 deg) and the vortex cores maintain their separate identity without merging into a single vortex, even at higher AOAs. This latter finding is in direct contrast to that reported in Refs. 7 and 10, and the numerical solutions[6,13] that show weak vortex interactions at low AOAs leading to merging and subsequent bursting at higher AOAs. The solutions of Kern[6] also reveal an unusual wing vortex structure midway down the leading edge of the wing, suggesting the presence of a second (torn) wing vortex. However, the available experimental evidence is too limited to substantiate this computational prediction.

More experimental studies are needed to investigate the resulting vortex structure on double-delta wings and to establish whether small deployable fillets could provide substantial control over the vortex core trajectory and bursting at high AOA during both static and dynamic (maneuvering) conditions with or without sideslip. To this end, an experimental program was conducted in the Naval Postgraduate School (NPS) water tunnel to visualize vortical flows on sharp-edged double-delta wing models with and without juncture fillets. The models included a 76-/40-deg cropped double-delta wing baseline model and its three derivatives with small geometry modifications (fillets) at the junction of the strake and wing leading edges. Extensive, dye-injection flow visualization methods were utilized to track vortex trajectories and vortex bursting for a range of model angles of attack, sideslip, and pitch rates. The flow visualization results presented in this article pertain to the zero sideslip case and should be of interest to researchers working on similar configurations, especially in view of the clean support system used. Additional details of the investigation appear in Refs. 14–17.

Experiment

Water-Tunnel Facility

The NPS water tunnel is a closed-circuit facility for studying a wide range of aerodynamic and fluid dynamic phenomena (Fig. 1). Its key design features are high flow quality, horizontal orientation, and continuous operation. The test section is 38 cm wide, 51 cm high, and 152 cm long. Water velocities of up to 30.5 cm/s with a turbulence intensity of <1% are possible in the test section. The dye-supply system for injecting color dyes consists of six pressurized color dyes using water soluble food coloring and is provided with individually routed lines from the dye reservoir to the model support system attached to the top of the tunnel (Fig. 2). The model is usually mounted upside down in the test section. The model support system utilizes a C-strut to vary the pitch travel up to 50 deg between the limits of −10 and 110 deg, and a turntable to provide yaw variations up to ±20 deg. The two servomotors of the model attitude control system provide independent control of model pitch and yaw with two rates.

Double-Delta Wing Models

The baseline double-delta wing model and its three derivatives used in the investigation are shown in Fig. 3. The models were constructed of 6.3-mm-thick Plexiglas® with a 76-deg sweep for the strake and a 40-deg sweep for the wing, both with sharp, bevelled leading edges and flat top surfaces. Each model has a C of 238 mm, a span of 241 mm, and an aspect ratio of 2.34. The geometry modification (fillet) at the intersection (juncture or kink) of the strake and wing leading edges on each derivative model increased the planform area of the

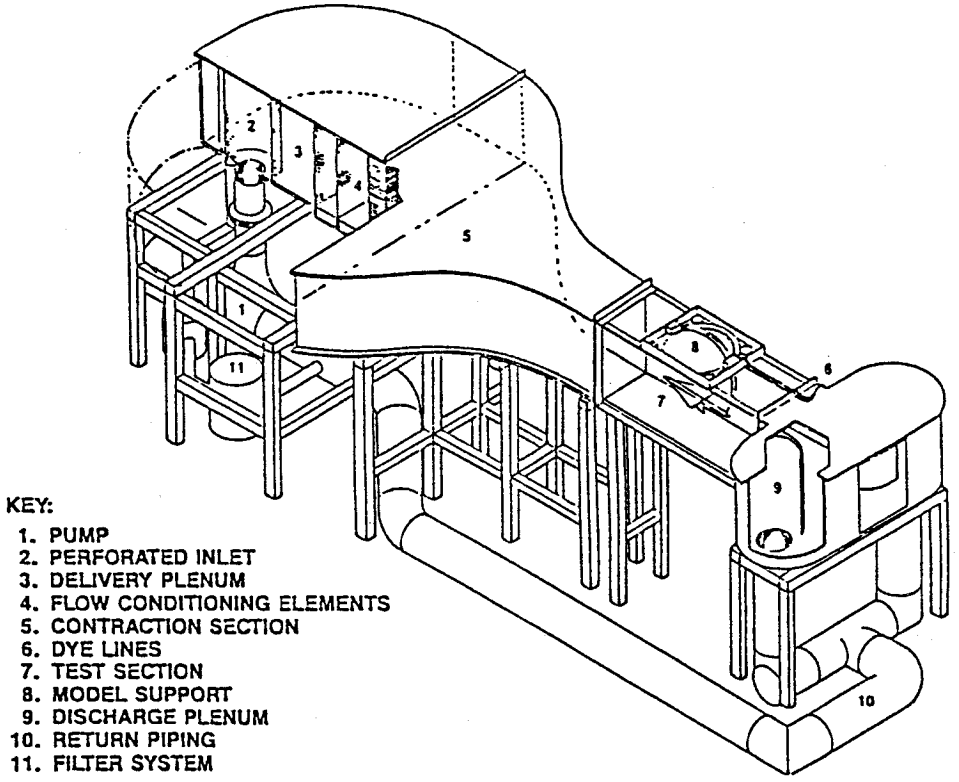

Fig. 1 NPS flow visualization water-tunnel facility.

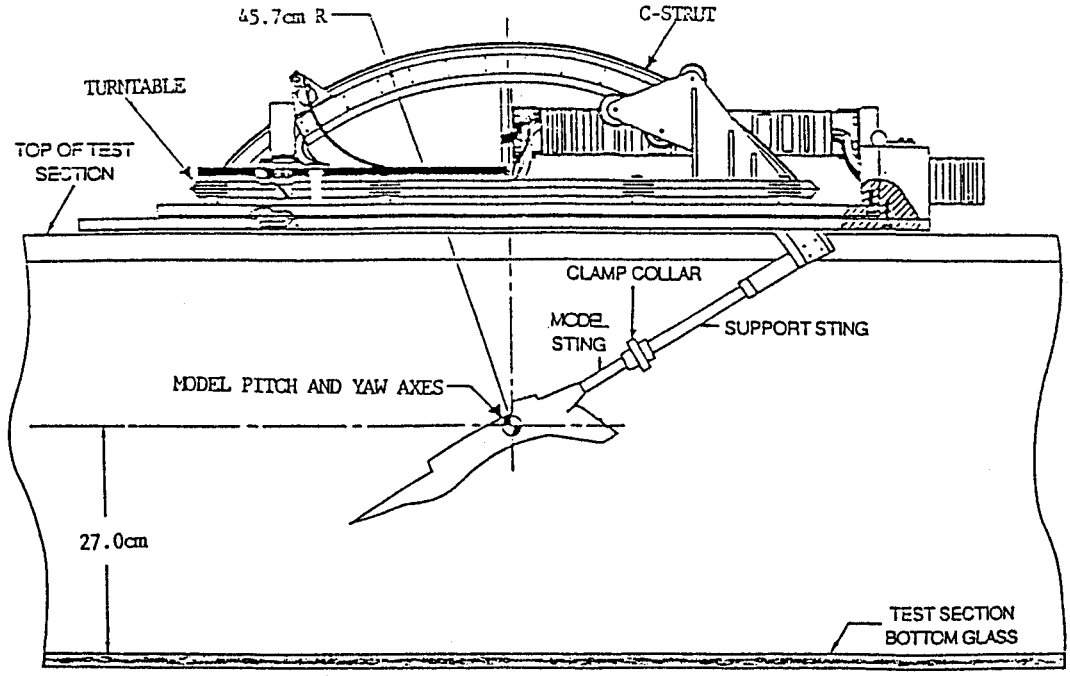

Fig. 2 Model support system of the NPS water tunnel.

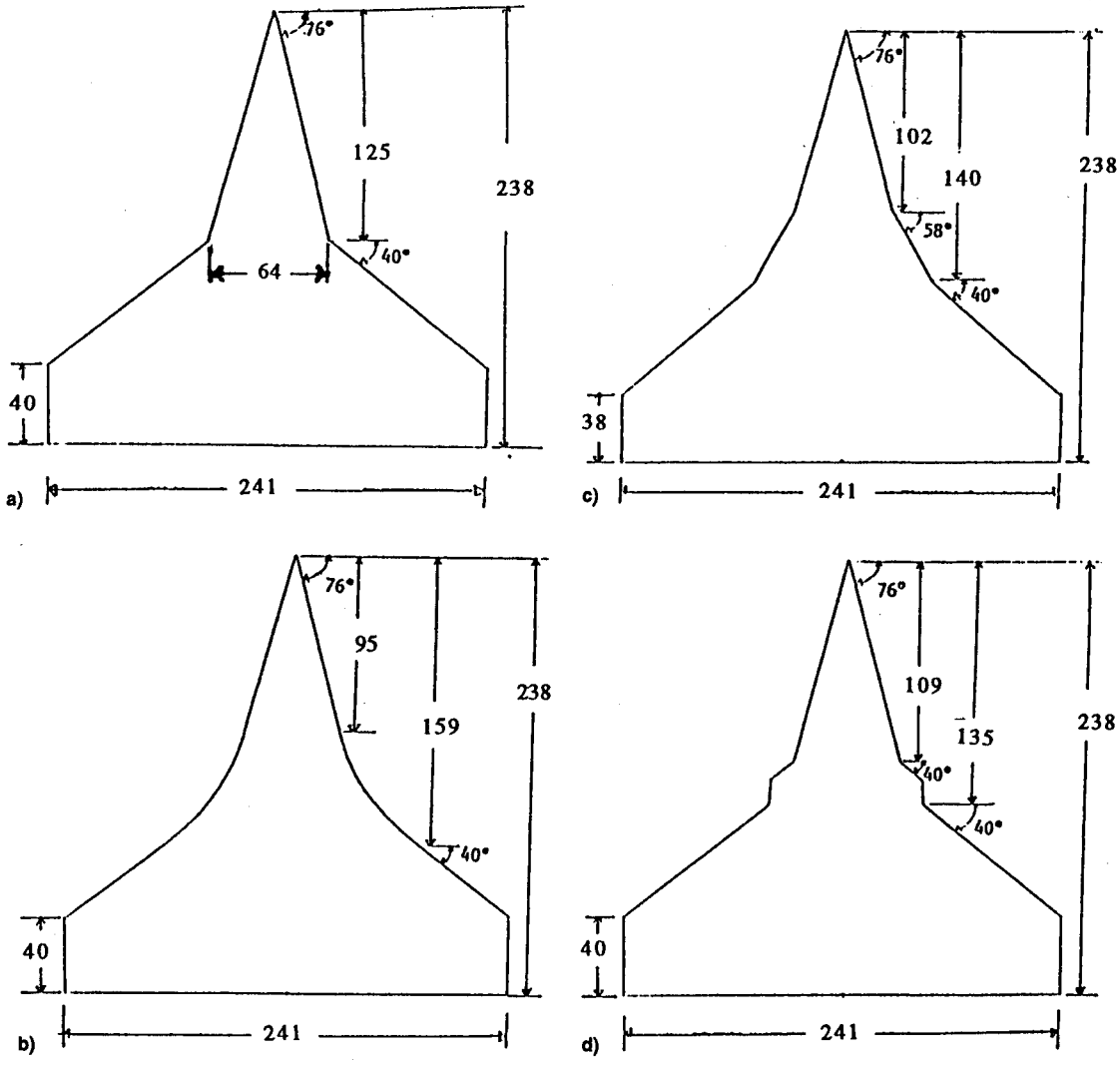

Fig. 3 Double-delta wing models: a) baseline (no fillet), b) parabolic-fillet, c) linear-fillet, and d) diamond-fillet models. All linear dimensions are in millimeters.

baseline model by 1%. The fillet dimensions are identical to the ones used by Kern.[6] The upper surface of the models had grid lines marked for easy identification of vortex core trajectory and burst location. The location of the dye-tube tip and the rate of dye-injection were crucial to obtain a good flow visualization of the vortical flowfield. Satisfactory dye injection for vortex visualization purposes was achieved by positioning small brass tubes flat on the model bottom surface with their tips very close to the vortex shedding points (viz., apex, kink, fillet), and adjusting the injection rate properly.

Experimental Program and Test Conditions

The experimental program was carried out in two phases. The first phase involved the visualization of vortex trajectory and breakdown on the upper surface of the static models for several AOAs at zero sideslip. The second phase involved the visualization of vortex breakdown on the upper surface of the pitching models at zero sideslip. During the static visualization the α was varied from 0 to 50 deg. During the dynamic visualization α varied from 0 to 50 deg (simple pitch-up motion) and 50 to 0 deg (simple pitch-down motion). The U_∞ in the tunnel was maintained at a nominal value of 7.6 cm/s, corresponding to a nominal Re of 1.875×10^4 based on the centerline chord. The $d\alpha/dt$ during the dynamic motion was ± 3.85 deg/s, yielding a reduced pitch rate of $k = \pm 0.1$. The model pitch axis was located 133 mm aft of the apex ($0.56C$). Both still-picture photography and videotape recording were used for documentation of dye-flow visualization of the model in both topview and sideview during static and dynamic conditions.

Results and Discussion

During the flow visualization study, the trajectories of the strake and wing vortices were easily recognized over the wing upper surface (see photographs in Ref. 17) as the dye fluid issuing out of the apex and kink locations exhibited features characteristic of a vortex core trajectory (viz., circumferential motion, bursting). Being a strong vortex, the identification of the strake vortex core was easier and straightforward. Detailed water flow visualization studies on 80-deg strake double-delta wing models with variable wing sweep (80–40 deg) reported by Thompson[10] clearly confirm the presence of the wing vortex for $Re \geq 1.5 \times 10^4$. As the Reynolds number in the present study exceeded this value, it reinforces the direct, visual interpretation of the dye line originating at the kink as representing a vortex core. In the following discussion the kink vortex of the baseline/fillet model is referred to as the wing vortex/fillet vortex, respectively.

Data reduction essentially consisted of measuring the vortex core locations in the X direction (along the model centerline from the apex), the Y direction (outboard from the model centerline), and the Z direction (perpendicular to and away from the surface) and plotting Y vs X and Z vs X to obtain trajectories at different AOAs. The aftmost point reported on the trajectory usually represented the last clearly identifiable core location before vortex breakdown. The vortex core locations were visually selected from the videotape/photographs in a careful, consistent manner and then nondimensionalized using the centerline chord length. Nevertheless, there will be some inaccuracies in the data because of the difficulty in assessing core locations associated with unsteady vortex bursting, particularly at high AOAs. In fact, during the static segment of the experiment (i.e., zero pitch rate) the breakdown location at any AOA fluctuated up to ± 19 mm (about $\pm 0.08C$); therefore, the reported values should be viewed as mean ones. It was extremely difficult to assess core locations of wing and fillet vortices when the AOA was higher than 30 deg, so there were no data for the wing and fillet vortices above 30 deg. Both the vortex trajectory data and the vortex breakdown location data are tabulated in Ref. 15.

The following sections briefly describe the behavior of the vortical flow and the effect of fillets, with emphasis on vortex interaction, vortex core trajectories, and vortex bursting.

Vortex Interaction

The vortex interaction phenomenon can be studied with the help of combined trajectory plots. Figures 4 and 5 show the interaction for the baseline model in the spanwise direction as a function of the streamwise location (X/C) at AOAs of 10 and 20 deg, respectively. At 10-deg AOA both the strake and the wing vortex cores are already well developed over the model and coiled up around each other (Fig. 4). The strake vortex core is nearly conical over the strake portion of the model ($X/C \leq 0.52$), but is drawn outboard by the wing vortex. At the same time, the wing vortex is drawn away from the wing leading edge by the strake vortex. The interaction or coiling-up between the strake vortex core and the wing vortex core starts at 64% of the centerline chord and 11% outboard from the model centerline. The vortex cores do not merge into a single vortex. The strake vortex bursts at $X/C = 0.93$ and the wing vortex bursts close to the trailing edge. As the AOA is increased further, the interaction occurs earlier and inboard and the burst locations move forward. At 20-deg AOA (Fig. 5), no vortex core intertwining (interaction) is possible as the strake vortex core bursts at $0.66C$ just ahead of the wing vortex. At 30-deg AOA, the strake vortex core bursts at $0.37C$ way ahead of the origin of the wing vortex.[17] Figure 6 is a combined trajectory plot for the baseline model showing the interaction in the normal direction at AOA = 10 deg. As the AOA is increased further, the interaction of the two vortices moves upward from the surface.[17]

The combined trajectory plots for the filleted models exhibit similar but more intense and complex interactions because of the formation of additional vortices in the fillet region. Compared to the baseline model the interaction is seen to persist over a larger range of AOA. For example, at 20-deg AOA of the diamond-fillet model, the strake vortex core interacts at $X/C = 0.525$ and $Y/C = 0.085$ with the beginning-of-fillet vortex core and at $X/C = 0.65$ and $Y/C = 0.12$ with the end-of-fillet vortex core (Fig. 7). However, at 30-deg AOA there is no interaction at all as the fillet vortices are already burst right at their origin, and therefore, there is only the strake vortex core present with its burst location ahead of the fillet location.[17] The vortex interaction does not exhibit any tendency toward vortex merging.

To summarize, the combined trajectory plots highlight the mutual induction effect of strake and wing vortex cores on each other. The strake vortex induces an upward and inboard movement of the wing vortex, and conversely, the wing vortex induces a downward and outboard movement of the strake vortex. The interaction of the two vortex cores leads to their intertwining (that is coiling around each other). With increasing AOA, the interaction moves upstream until strake vortex bursting occurs even before the interaction with the wing vortex. These observations are in general agreement with those reported in Refs. 8–11. Over the range of the present investigation it is seen that the AOA range for coiling-up of the vortices is quite narrow (approximately 10–20 deg), and even at higher AOAs the vortex cores maintain their separate identity without merging into a single vortex. This finding is in qualitative agreement with that reported in Refs. 8, 9, and 11, but disagrees with the earlier investigations of Verhaagen[7] and Thompson[10] and the more recent wind-tunnel investigation of Verhaagen et al.[18]

While comparing the data from different sources it is important to be aware of the several parameters that might influence the data. It is known that the vortex interaction on the upper surface of double-delta wings depends on several parameters, including model geometry (leading-edge sweep angles, edge shapes, kink location, wing cropping, etc.), AOA, and flow Reynolds number. The flow conditions used here and in

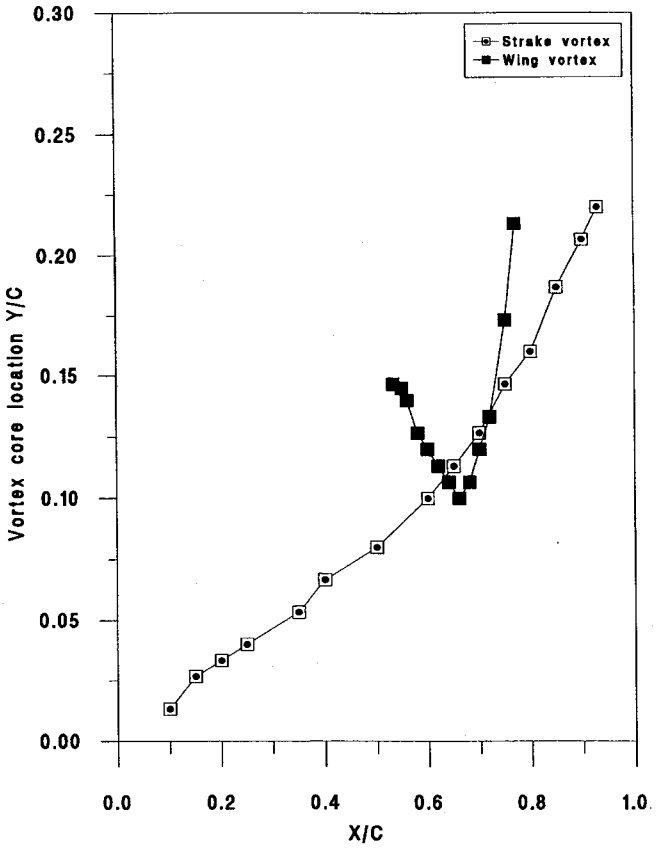

Fig. 4 Vortex core location *Y/C* for baseline model at AOA = 10 deg.

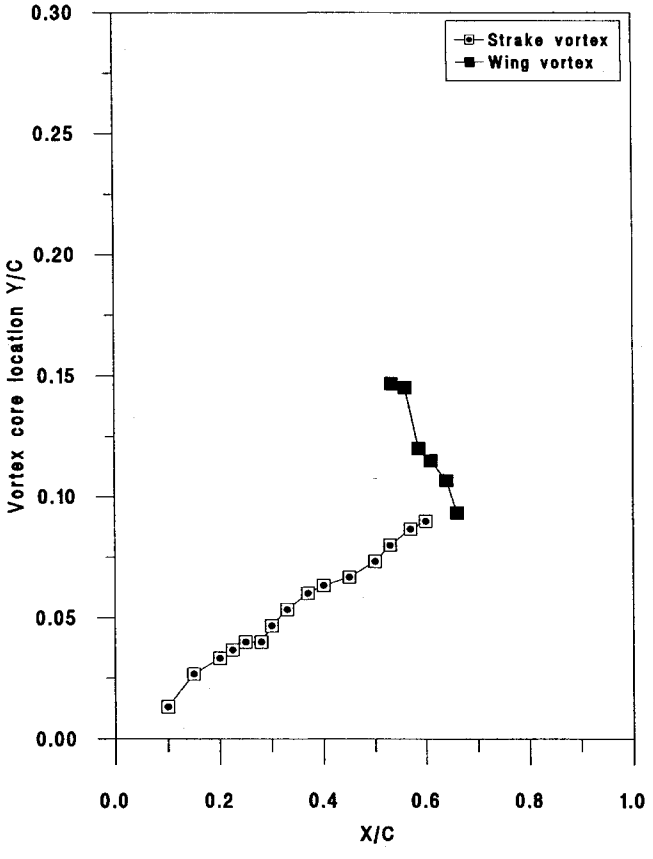

Fig. 5 Vortex core location *Y/C* for baseline model at AOA = 20 deg.

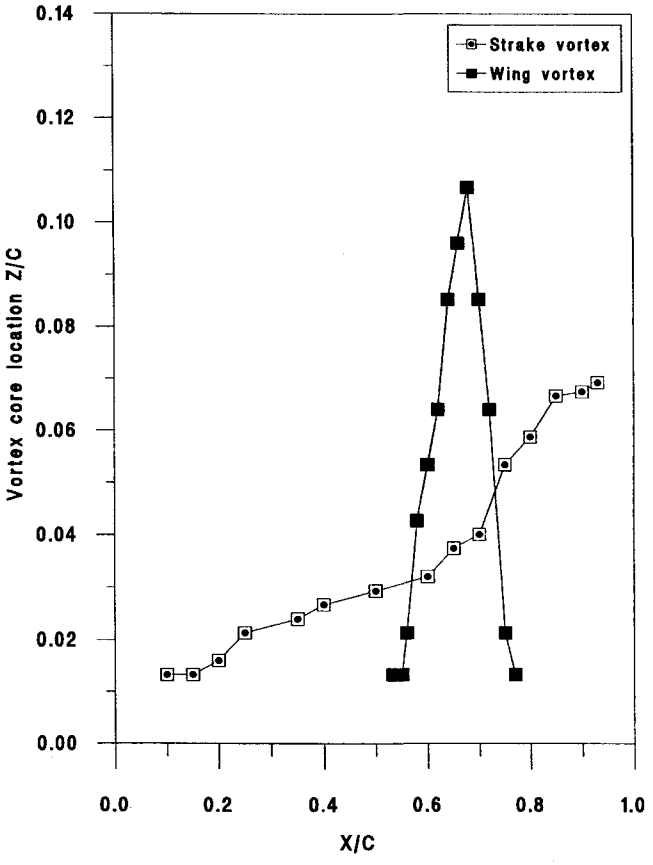

Fig. 6 Vortex core location *Z/C* for baseline model at AOA = 10 deg.

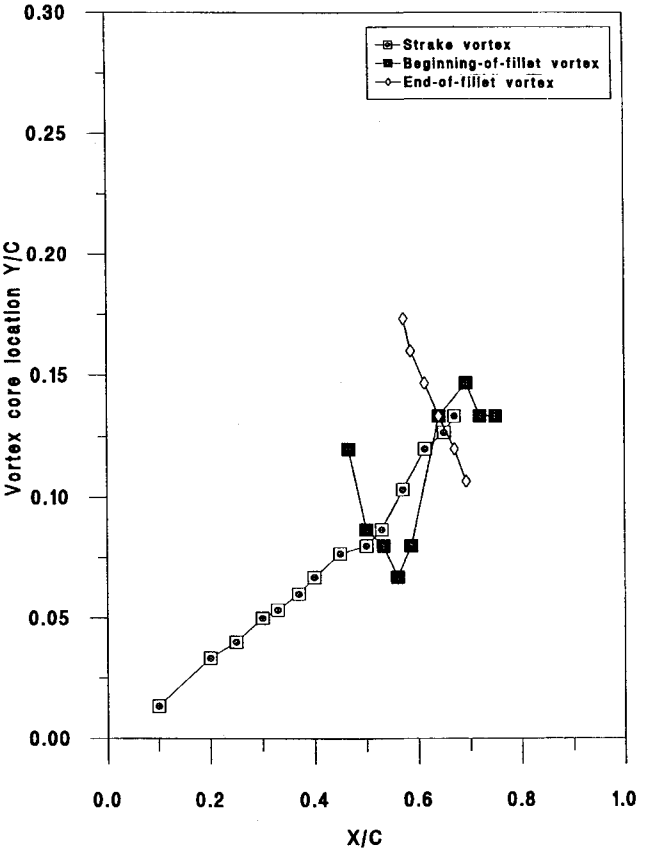

Fig. 7 Vortex core location *Y/C* for diamond-fillet model at AOA = 20 deg.

Ref. 11 were identical and the baseline models differed only in the trailing-edge shape. While both the geometry and the flow conditions of the baseline model used here did not exactly match with those in Refs. 7–10, the model geometry closely approximated that used in Refs. 6 and 18. The flow Reynolds number of the present study was quite low, by about two orders of magnitude compared to the values quoted in Refs. 6 and 18 ($Re = 1 \times 10^6$). The numerical solutions[5] predict weak vortex interaction at low AOAs leading to merging and subsequent bursting at higher AOAs. The wind-tunnel data[18] for the baseline model imply that the wing vortices burst earlier than the strake vortices and there is no vortex interaction (intertwining or coiling-up) and no merging. However, the present data for the baseline model indicate vortex interaction over a narrow AOA range, earlier bursting of the strake vortices and no merging at all, thus contradicting the findings of both Refs. 6 and 18 and raising the question whether this disagreement is caused by the Reynolds number difference. At low Reynolds numbers the shed wing vortices are weak and are therefore greatly influenced by the stronger strake vortex. As shown by Thompson,[10] high Reynolds number water-tunnel data will better reflect the wind-tunnel and full-scale data. In a recent laser-Doppler and dye visualization study of the same configuration the Reynolds number was varied from 1.5×10^4 to quadruple this value. It was found that the strake and wing vortex behavior started to approach that reported by Verhaagen et al.[18] as the Reynolds number was increased. The detailed findings of this investigation are documented in Ref. 19.

Vortex Core Trajectories

Figures 8–10 illustrate the effect of AOA on individual vortex core trajectories for the baseline model. The nondimensional $X-Y$ and $X-Z$ plots shown in Figs. 8 and 9 for the strake vortex trajectory clearly indicate that, as expected, with increasing AOA the strake vortex core burst point moves up-

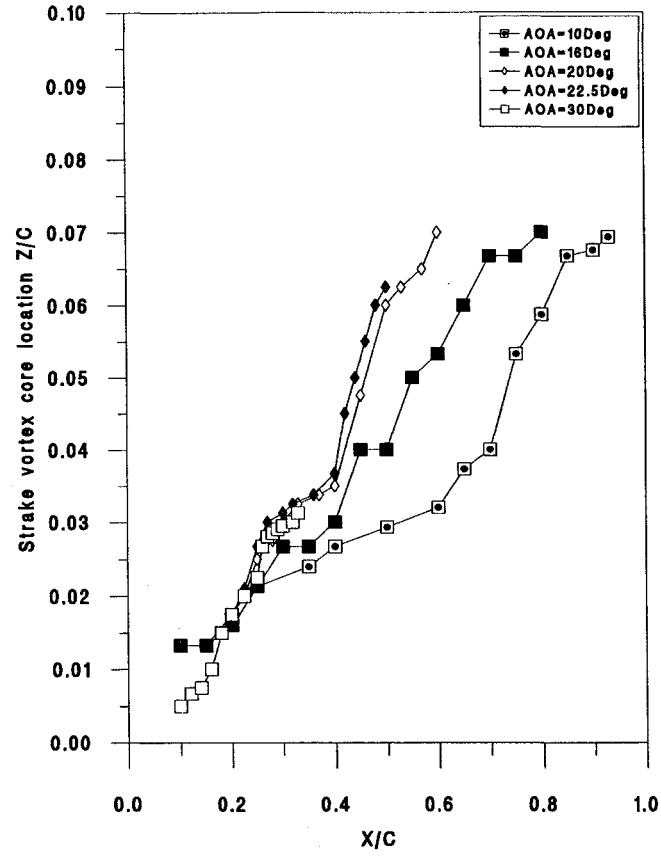

Fig. 9 Strake vortex core location Z/C for baseline model at different AOAs.

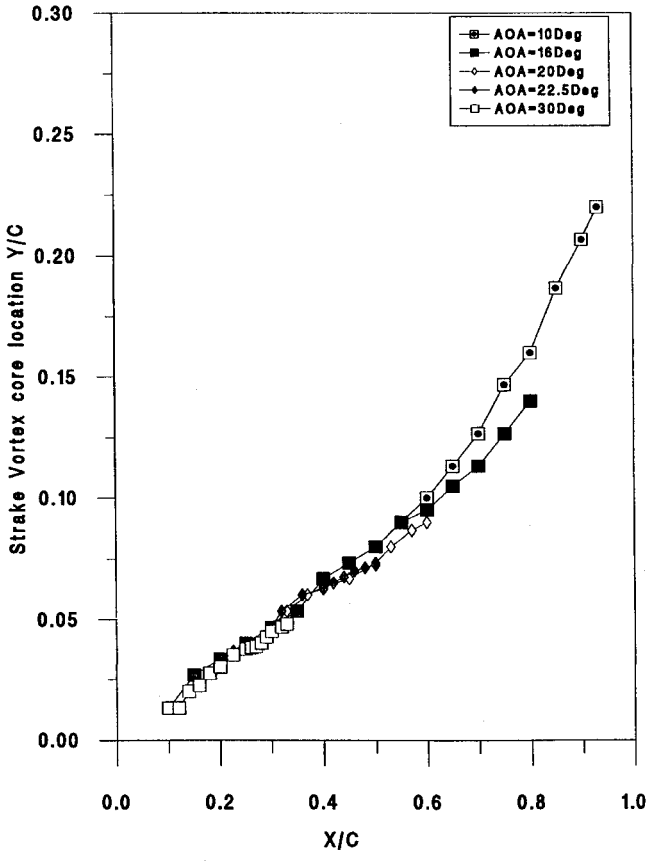

Fig. 8 Strake vortex core location Y/C for baseline model at different AOAs.

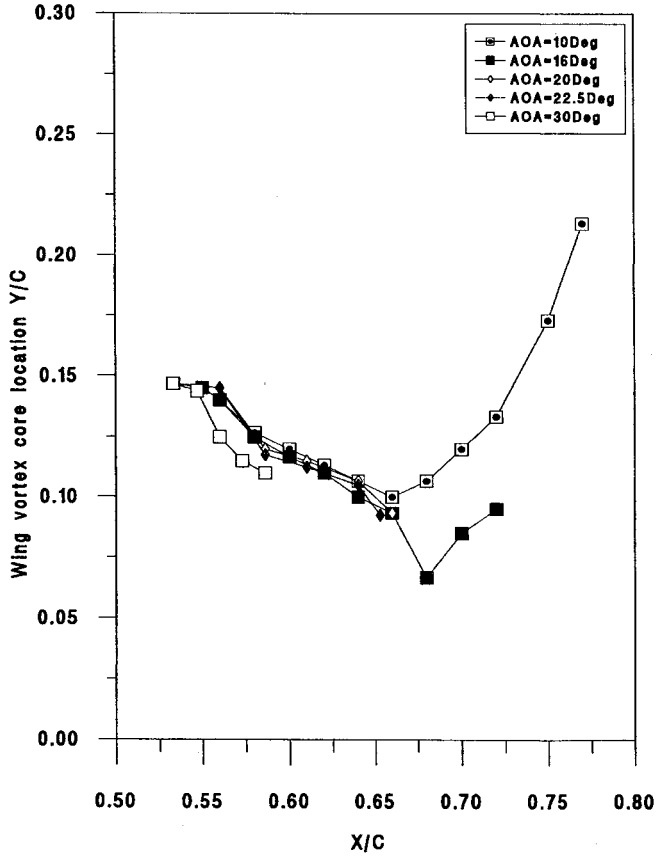

Fig. 10 Wing vortex core location Y/C for baseline model at different AOAs.

stream (see discussion on vortex bursting), the vortex core moves inboard and away from the surface. The wing vortex core burst point also moves upstream with increasing AOA, as seen in Fig. 10, but the trajectory movements in the spanwise and normal directions are clearly not monotonic because of strong interaction, particularly at low AOAs. Similar trends have been observed in the trajectory plots for the filleted models.[15,17]

Figures 11–14 show the effect of fillet shape on strake vortex core trajectories. Figures 11 and 12 represent the strake vortex core location in the *Y* direction for AOAs of 10 and 20 deg, respectively. At 10-deg AOA the strake vortex core of the baseline model is closer to the model centerline than those of the filleted models. As the AOA increases from 10 to 20 deg the vortex cores move inboard for all of the models. Similar trends are also observed at 30-deg AOA (Ref. 17). Compared to the baseline model, the filleted models indicate a smaller inboard movement of the vortex core. Figures 13 and 14 represent the strake vortex core location in the *Z* direction for AOAs of 10 and 20 deg, respectively. These plots highlight that for all test AOAs, the vortex core trajectories of the baseline model are among those farthest from the surface, whereas the trajectories for the diamond-fillet model are among those closest to the surface. It is also noticed from these trajectory plots that at any given AOA, the strake vortex core of the diamond-fillet model exhibits a more persistent vortex (i.e., largest *X/C* value). Thus, the strake vortex of the diamond-fillet model has a longer core length that remains closer to the surface, but farther out from the centerline chord. This qualitatively implies an improved flowfield over the wing surface, and consequently, lift augmentation.

Vortex Core Breakdown (Bursting)

A detailed discussion of the strake vortex burst response during both static and dynamic pitching conditions of the base-

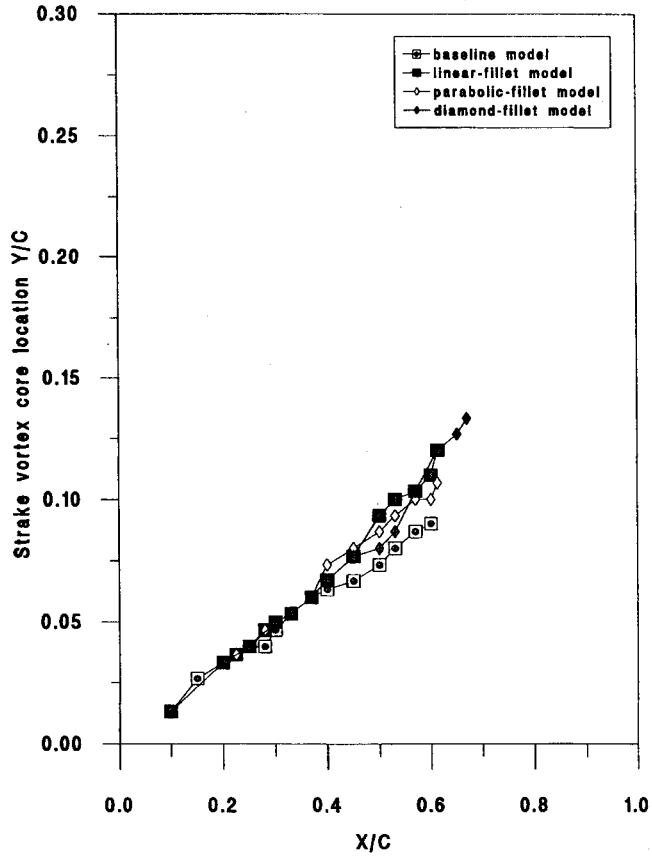

Fig. 12 Effect of fillet shape on strake vortex core location *Y/C* at AOA = 20 deg.

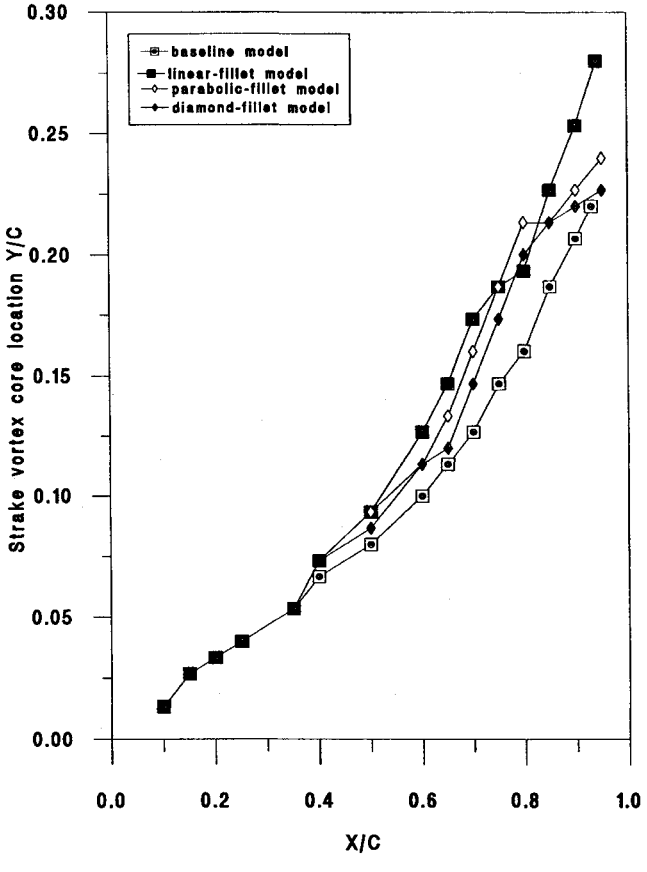

Fig. 11 Effect of fillet shape on strake vortex core location *Y/C* at AOA = 10 deg.

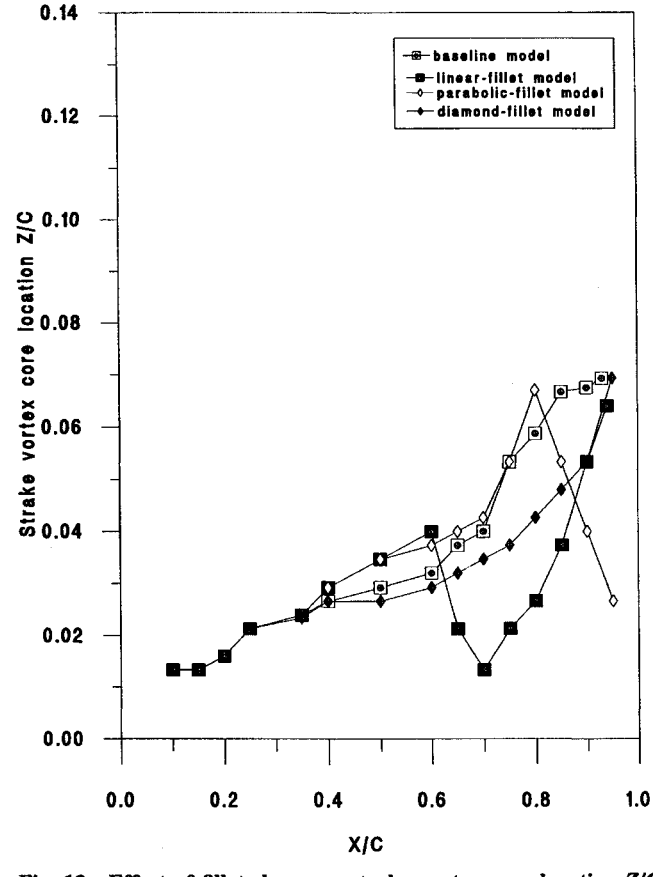

Fig. 13 Effect of fillet shape on strake vortex core location *Z/C* at AOA = 10 deg.

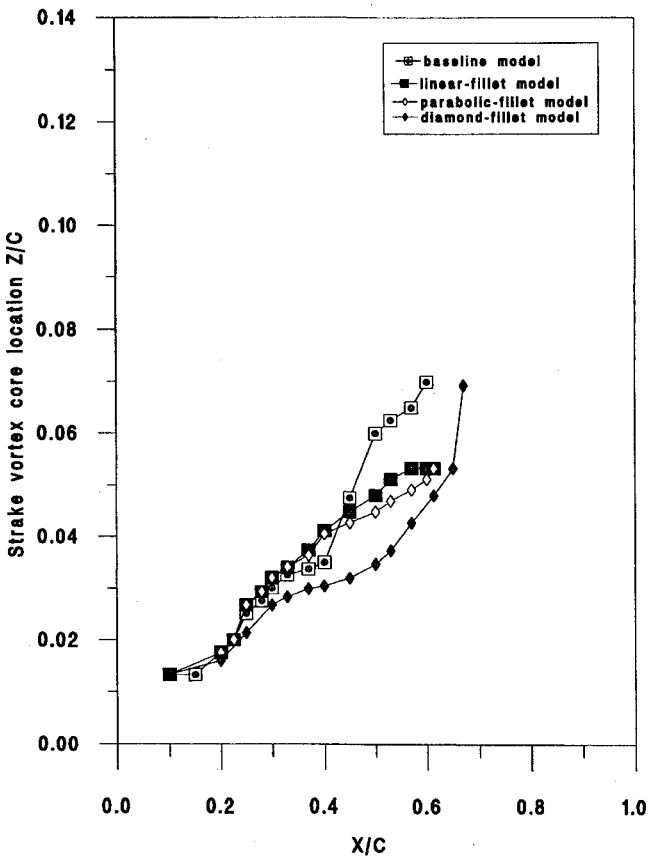

Fig. 14 Effect of fillet shape on strake vortex core location *Z/C* at AOA = 20 deg.

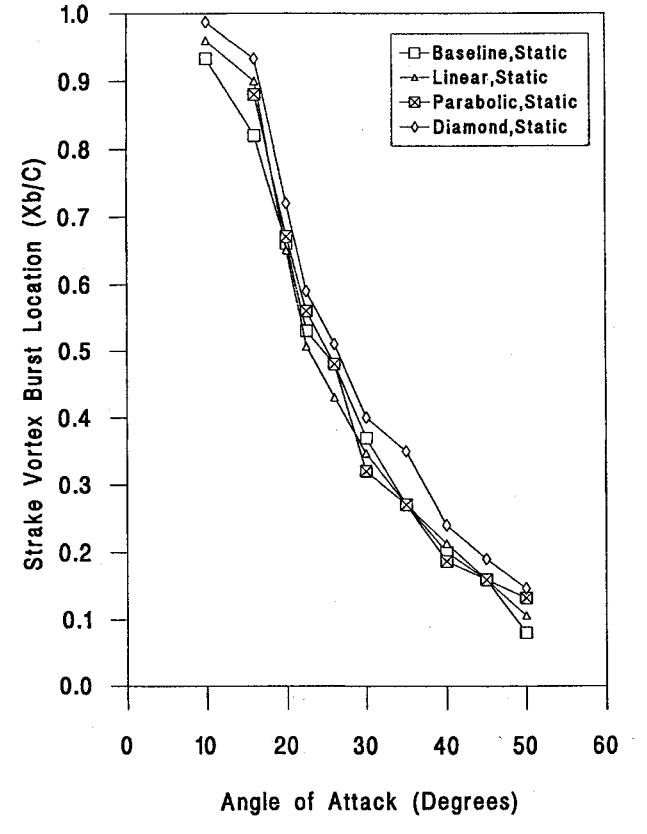

Fig. 15 Effect of fillet shape on strake vortex burst location for static condition.

line and filleted models appears in Refs. 14 and 15. The vortex burst response and the dynamic lag effects associated with the pitching motion are very similar to the ones reported in various experimental investigations on delta wings,[20] double-delta wings,[8,11] and aircraft models.[21,22] To see the effect of fillet shapes on vortex core breakdown, composite burst location plots were prepared by superposing individual burst location plots for different models. Figure 15 compares the static burst location plots showing the longitudinal location of the bursting of the strake–vortex core X_b as a function of AOA in the 10–50-deg AOA range. It is important to consider the experimental uncertainty associated with the measurements. While no definite trend in the vortex burst response of parabolic-fillet and linear-fillet models relative to the baseline model is detectable over the AOA range tested, the results indicate a clear trend in the vortex burst delay for the diamond-fillet shape. Any delay in burst location is likely to improve the flowfield over the wing surface and therefore implies lift augmentation. Thus the previous data correlate well with the numerical prediction of Kern,[6] verifying the concept for flow control by fillets for the static case.

Figure 16 compares the dynamic burst location plots of different fillet shapes with that of the baseline model. A close examination of the dynamic curves of the pitch-up case reveals the same trend as discussed previously for the static case. In particular, a clear trend in the vortex burst delay is indicated for the diamond-fillet model. However, during the pitch-down motion, all three fillet shapes indicate a vortex burst delay compared to the baseline model. The data therefore imply possible lift augmentation with diamond fillet shape during pitching maneuvers, extending the concept of flow control by fillets to dynamic maneuvering conditions.

Thus the flow visualization data have verified the concept of flow control by fillets for both static and dynamic conditions. Force balance data are certainly needed to completely validate the concept on a quantitative basis and for direct comparison with the numerical predictions.[6]

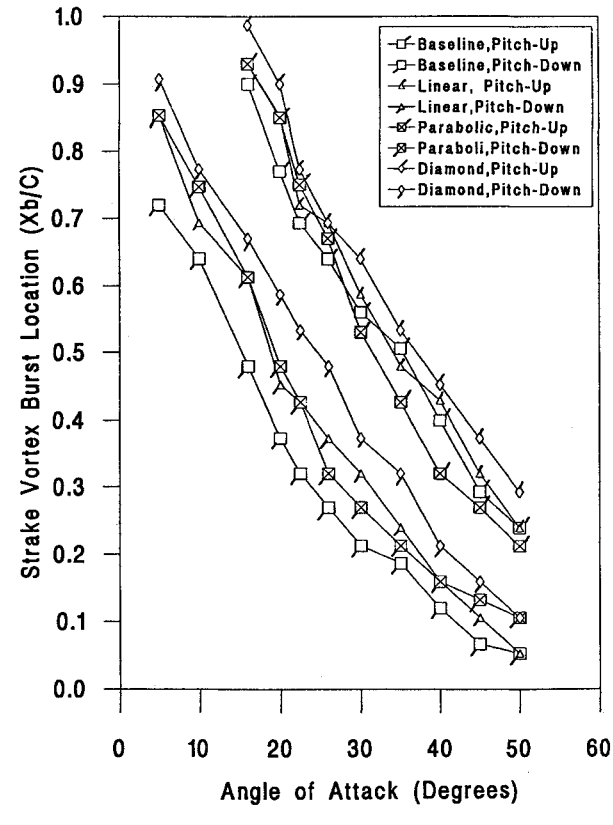

Fig. 16 Effect of fillet shape on strake vortex burst location during dynamic (pitching) motion.

Conclusions

A water-tunnel flow visualization study was conducted to investigate the effect of juncture fillets on the vortical flow over a cropped, double-delta wing model with sharp leading edges. The study focused on vortex interaction, vortex core trajectories, and vortex breakdown on the leeward surface at high AOAs with zero sideslip. The following conclusions are based on the results of the experimental investigation at $Re = 1.875 \times 10^4$.

1) The mutual induction effect of strake and wing/fillet vortex cores on each other leads to their intertwining (i.e., coiling around each other). With increasing AOA, the interaction point moves upstream, inboard, and upward, but only until the AOA is large enough to cause the bursting of the strake vortex even before the interaction could begin.

2) The vortex interaction is limited to low AOAs in the range 10–20 deg (or a little higher for a filleted model) with the strake vortex bursting earlier than the wing vortex; vortex merging does not take place even at higher AOAs.

3) The presence of fillets causes delay in both vortex interaction and vortex breakdown at high AOAs.

4) Compared to other models, the static data for the strake vortex trajectory of the diamond-fillet model indicate a clear improvement in vortex burst delay and consequently longer core length, with the core remaining closest to the surface and farthest from the centerline at high AOAs. These features imply lift augmentation and support the concept of flow control using fillets.

5) The dynamic data also clearly indicate a vortex burst delay for the diamond-fillet shape during both pitch-up and pitch-down maneuvers, extending the concept of using fillets for enhanced maneuverability of fighter aircraft.

Acknowledgments

This work was supported by the U.S. Naval Air Warfare Center/Aircraft Division, Warminster, Pennsylvania. The technical discussions with Steve Kern are acknowledged. The authors sincerely thank Ron Ramaker for fabricating the models.

References

[1]Lamar, J. E., "Nonlinear Lift Control at High Speed and High Angle of Attack Using Vortex Flow Technology," *Special Course on Fundamentals of Fighter Aircraft Design*, AGARD-R-740, Oct. 1987, pp. 4.1–4.23.

[2]Lamar, J. E., "Prediction of Vortex Flow Characteristics of Wings at Subsonic and Supersonic Speeds," *Journal of Aircraft*, Vol. 13, No. 7, 1976, pp. 490–494.

[3]Barlett, G. E., and Vidal, R. J., "Experimental Investigation of Influence of Edge Shape on the Aerodynamic Characteristics of Low Aspect Ratio Wings at Low Speeds," *Journal of the Aeronautical Sciences*, Vol. 22, No. 8, 1955, pp. 517–534.

[4]Rao, D. M., "Vortical Flow Management for Improved Configuration Aerodynamics—Recent Experiences," *AGARD Symposium on Aerodynamics of Vortical Type Flows in Three Dimensions*, CP-342, AGARD, Rotterdam, The Netherlands, April 1983 (Paper 30).

[5]Rao, D. M., and Campbell, J. F., "Vortical Flow Management Techniques," *Progress in Aerospace Sciences*, Vol. 24, No. 3, 1987, pp. 173–224.

[6]Kern, S., "Vortex Flow Control Using Fillets on a Double-Delta Wing," *Journal of Aircraft*, Vol. 30, No. 6, 1993, pp. 818–825; also AIAA Paper 92-0411, Jan. 1992.

[7]Verhaagen, N. G., "An Experimental Investigation of the Vortex Flow over Delta and Double-Delta Wings at Low Speed," Delft Univ. of Technology, Rept. LR-372, Delft, The Netherlands, Sept. 1983.

[8]Olsen, P., and Nelson, R., "Vortex Interaction over Double-Delta Wings at High Angles of Attack," AIAA Paper 89-2191, July 1989.

[9]Graves, T. V., Nelson, R. C., Schwimley, S. L., and Ely, W. L., "Aerodynamic Performance of Strake Wing Configurations," *High Angle-of-Attack Technology*, Vol. I, NASA CP-3149, Pt. I, May 1992, pp. 173–204.

[10]Thompson, D. H., "Visualization of Vortex Flow Around Wings with Highly Swept Leading Edges," 9th Australian Fluid Mechanics Conf., Auckland, Dec. 1986.

[11]Hebbar, S. K., Platzer, M. F., and Li, F. H., "A Visualization Study of the Vortical Flow over a Double-Delta Wing in Dynamic Motion," AIAA Paper 93-3425, Aug. 1993.

[12]Hsu, C. H., and Liu, C. H., "Upwind Navier-Stokes Solutions for Leading-Edge Vortex Flows," AIAA Paper 89-0265, Jan. 1989.

[13]Ekaterinaris, J. A., Coutley, R. L., Schiff, L. B., and Platzer, M. F., "Numerical Investigation of High Incidence Flow over a Double-Delta Wing," *Journal of Aircraft*, Vol. 32, No. 3, 1995, pp. 457–463.

[14]Hebbar, S. K., Platzer, M. F., and Alkhozam, A. M., "Investigation into the Effects of Juncture Fillets on the Vortical Flow over a Cropped, Double-Delta Wing," AIAA Paper 94-0626, Jan. 1994.

[15]Alkhozam, A. M., "Interaction, Bursting, and Control of Vortices of a Cropped Double-Delta Wing at High Angle of Attack," M.S. Thesis, U.S. Naval Postgraduate School, Monterey, CA, March 1994.

[16]Chang, W. H., "Effect of Juncture Fillets on Double-Delta Wings Undergoing Sideslip at High Angles of Attack," M.S. Thesis, U.S. Naval Postgraduate School, Monterey, CA, Sept. 1994.

[17]Hebbar, S. K., Platzer, M. F., and Alkhozam, A. M., "Experimental Investigation of Vortex Flow Control Using Juncture Fillets on a Cropped Double-Delta Wing," AIAA Paper 95-0649, Jan. 1995.

[18]Verhaagen, N. G., Jenkins, L. N., Kern, S. B., and Washburn, A. E., "A Study of the Vortex Flow over a 76/40-deg Double-Delta Wing," AIAA Paper 95-0650, Jan. 1995.

[19]Fritzelas, A., "A Water Tunnel Investigation of the Influence of Reynolds Number on the High-Incidence Flow over Double-Delta Wings," M.S. Thesis in Aeronautical Engineering, U.S. Naval Postgraduate School, Monterey, CA, March 1996.

[20]Magness, R. D., and Rockwell, D., "Control of Leading Edge Vortices on a Delta Wing," AIAA Paper 89-0900, March 1989.

[21]Hebbar, S. K., Platzer, M. F., and Cavazos, O. V., "Pitch Rate/Sideslip Effects on Leading Edge Extensions Vortices of an F/A-18 Aircraft Model," *Journal of Aircraft*, Vol. 29, No. 4, 1992, pp. 720–723.

[22]Hebbar, S. K., Platzer, M. F., and Kwon, H.-M., "Vortex Breakdown Studies of a Canard-Configured X-31A-Like Fighter Aircraft Model," *Journal of Aircraft*, Vol. 30, No. 3, 1993, pp. 405–408.